Vol. 35, No. 1 (2013) 25-35

Tribology in Industry

www.tribology.fink.rs

RESEARCH

Mechanical Properties and Corrosion Behaviour of Aluminium Hybrid Composites Reinforced with Silicon Carbide and Bamboo Leaf Ash

K.K. Alaneme[a], B.O. Ademilua[a], M.O. Bodunrin[a]

[a]Department of Metallurgical and Materials Engineering, Federal University of Technology, Akure, P.M.B 704, Nigeria.

Keywords:

Hybrid composites
Bamboo leaf ash
Al-Mg-Si alloy
Corrosion
Stir casting
Mechanical properties
Silicon carbide

Corresponding author:

Kenneth K. Alaneme
Department of Metallurgical and Materials Engineering,
Federal University of Technology, Akure, P.M.B 704, Nigeria
E-mail: kkalaneme@gmail.com

A B S T R A C T

The viability of developing low cost – high performance Al matrix hybrid composites with the use of bamboo leaf ash (an agro waste ash) and silicon carbide as complementing reinforcements was investigated. Silicon carbide (SiC) particulates added with 0, 2, 3, and 4 wt% bamboo leaf ash (BLA) were utilized to prepare 10 wt% of the reinforcing phase with Al-Mg-Si alloy as matrix using two-step stir casting method. Microstructural characterization, mechanical properties evaluation and corrosion behaviour were used to assess the performance of the composites. The results show that the hardness, ultimate tensile strength, and percent elongation of the hybrid composites decrease with increase in BLA content. The fracture toughness of the hybrid composites were however superior to that of the single reinforced Al - 10 wt% SiC composite. Only the 2 wt% BLA containing hybrid composite had specific strength value comparable to that of the single reinforced composite. In 5wt% NaCl solution, it was observed that the 2 and 3 wt % BLA containing hybrid composites had higher corrosion resistance in comparison to the single reinforced Al - 10 wt% SiC composite but the reverse trend was observed in 0.3 M H_2SO_4 solution where the single reinforced had superior corrosion resistance.

1. INTRODUCTION

The synthesis and characterization of a wide range of Aluminium based composites has continued to generate a lot of interest judging from the large volume of publications in this area of materials science and engineering for the past thirty years [1-3]. This is due to the versatile applications Al based composites have been successfully utilized in and the huge prospects it has for so many other new applications [3-4]. From the development of high performance components for automobile, aerospace, defense, marine and other notable industrial applications to the development of facilities for sports and recreation [5-7], the areas of application of Al based composites is expected to still continue to grow. This is possible by virtue of the attractive property spectrum possessed by AMCs and the lower cost of production in comparison with other competing MMCs or engineering materials for similar applications [8-9].

The selection of reinforcing material for Al matrices is very important in ensuring that desired property combinations are harnessed [10]. The target for most developing countries involved in AMCs development is optimizing cost reduction and performance levels by consideration of industrial and agro wastes as reinforcing materials. This philosophy is informed by the relatively high cost of purchasing the commonly used synthetic reinforcements such as silicon carbide and alumina from abroad [11]. Fly ash, silica, and graphite are a few examples of industrial/inorganic materials that have been used as reinforcement in AMCs [12-14]. Rice hush ash, bagasse ash, and coconut shell ash are a few agro waste products which have also been tested as potential reinforcing material [11, 15,16]. Though literatures on the potentials of agro-waste ashes are still scanty (compared to the synthetic reinforcement), the available results show that Al based composites reinforced with synthetic ceramics such as silicon carbide and alumina have superior properties in comparison to the agro waste ash reinforced grades [17]. An approach which will seek to harness the clearly superior strength levels of the synthetic reinforcements and the lower cost and density advantages of the agro wastes have not received much attention in literature. This research work is motivated by the prospect of developing high performance Al matrix hybrid composites using silicon carbide and bamboo leaf ash as complementing reinforcements. Bamboo trees are found in large quantities in Nigeria and likewise so many other parts of the world; and the leaves often liter the environments where they are found [18]. Management of most agro wastes could be overwhelming and the best approach remains to explore more recycling techniques; and then applications where recycled wastes can be productively utilized. This work is part of current efforts aimed at considering the potentials of a wide range of agro waste ashes for the development of low cost-high performance Aluminium based hybrid composites. These low cost hybrid composites could have potentials for use in stress bearing and wear applications among others [15]. In this paper, the processing, microstructural features, mechanical and corrosion behavior of an Al matrix composite reinforced with varied weight ratios of bamboo leaf ash and silicon carbide is reported.

2. MATERIALS AND METHOD

2.1 Materials

Al-Mg-Si alloy with chemical composition presented in Table 1 was selected as Al matrix for the investigation. Chemically pure silicon carbide (SiC) particles having average particle size of 30 μm and processed ash (<50 μm) derived from controlled burning and sieving of dry bamboo leaves were used as reinforcement for the Al matrix. Magnesium was procured for use in improving wettability between the Al matrix and the reinforcements.

Table 1. Elemental composition of Al-Mg-Si alloy.

Element	wt%
Si	0.4002
Fe	0.2201
Cu	0.008
Mn	0.0109
Mg	0.3961
Cr	0.0302
Zn	0.0202
Ti	0.0125
Ni	0.0101
Sn	0.0021
Pb	0.0011
Ca	0.0015
Cd	0.0003
Na	0.0009
V	0.0027
Al	98.88

2.2 Preparation of Bamboo Leaf Ash

Dry bamboo leaves were gathered from the environs of farm lands near the University Campus having a large mass of bamboo trees. The bamboo leaves were placed in a metallic drum and fired in open air to allow for thorough combustion. The ash produced from the burning process was allowed to cool for 24 hours before removal from the drum. The ash was then conditioned using a furnace at a temperature of 650 ^{o}C for 3 hours in accordance with [18]. Sieving of the bamboo leaf ash was then performed using a sieve shaker to obtain ashes with mesh size under 50 μm. The chemical composition of the bamboo leaf ash is presented in Table 2.

Table 2. Chemical composition of Bamboo Leaf Ash.

Compound/Element (constituent)	weight Percent
Silica (SiO2)	75.9
Aluminium oxide, Al_2O_3	4.13
Calcium oxide CaO	7.47
Magnesium oxide, MgO	1.85
Potassium oxide, K_2O	5.62
Haematite, Fe_2O_3	1.22
Titanium oxide, TiO_2	0.20

2.3 Production of Composites

Two steps stir casting process performed in accordance with Alaneme and Aluko [19] was adopted for the production of the composites. Charge calculation was used to determine the amount of bamboo leaf ash (BLA) and silicon carbide (SiC) required to prepare 10 wt% reinforcements (in the Al matrix) consisting of 0:10, 2:8, 3:7, and 4:6 bamboo leaf ash and silicon carbide weight percents respectively. The bamboo leaf ash and silicon carbide particles were initially preheated separately at a temperature of 250 °C to remove moisture and to help improve wettability with the molten Al-Mg-Si alloy. The Al-Mg-Si alloy billets were charged into a gas-fired crucible furnace (fitted with a temperature probe), and heated to a temperature of 750 °C ± 30 °C (above the liquidus temperature of the alloy) to ensure the alloy melts completely. The liquid alloy was then allowed to cool in the furnace to a semi solid state at a temperature of about 600 °C. The preheated bamboo leaf ash and Sic particles along with 0.1 wt% magnesium were then charged into the melt at this temperature and stirring of the slurry was performed manually for 5-10 minutes. The composite slurry was superheated to 800 °C ± 50 °C and a second stirring performed using a mechanical stirrer. The stirring operation was performed at a speed of 400 rpm for 10 minutes before casting into prepared sand moulds inserted with chills.

2.4 Density Measurement

The densities of the composites were determined by comparing the experimental and theoretical densities of each composition of the BLA-SiC reinforced composites produced [19]. The experimental density was determined by dividing the measured weight of a test sample by its measured volume; while the theoretical density was evaluated by using the rule of mixtures given by:

$$\rho_{Al\text{-}Mg\text{-}Si\,/\,BLA\text{-}SiCp} = wt._{Al\text{-}Mg\text{-}Si} \times \rho_{Al\text{-}Mg\text{-}Si} + wt._{BLA} \times \rho_{BLA} + wt._{SiC} \times \rho_{SiC} \quad (2.1)$$

Where, $\rho_{Al\text{-}Mg\text{-}Si\,/\,BLA\text{-}SiCp}$ = Density of Composite, $wt._{Al\text{-}Mg\text{-}Si}$ = Weight fraction of Al-Mg-Si alloy, $\rho_{Al\text{-}Mg\text{-}Si}$ = Density of Al-Mg-Si alloy, $wt._{BLA}$ = Weight fraction BLA, ρ_{BLA} = Density of BLA, $wt._{SiC}$ = Weight fraction SiC, and ρ_{SiC} = Density of SiC.

The percent porosity of the composites was evaluated using the relations [20]:

$$\%\ porosity = \{(\rho_T - \rho_{EX}) \div \rho_T\} \times 100\% \quad (2.2)$$

where, ρ_T = Theoretical Density (g/cm^3), ρ_{EX} = Experimental Density (g/cm^3).

2.5 Tensile test

Tensile tests were performed on the composites produced in accordance with the specifications of ASTM 8M-91 standards [21]. The samples for the test were machined to round specimen configuration with 6 mm diameter and 30 mm gauge length. The test was carried out at room temperature using an Instron universal testing machine operated at a strain rate of 10^{-3}/s. Three repeat tests were performed for composite composition to guarantee reliability of the data generated. The tensile properties evaluated from the stress-strain curves developed from the tension test are - the ultimate tensile strength (σ_u), the 0.2% offset yield strength (σ_y), and the strain to fracture (ε_f).

2.6 Fracture Toughness Evaluation

The fracture toughness of the composites was evaluated using circumferential notch tensile (CNT) specimens in accordance with Alaneme [22]. The effectiveness of CNT testing for fracture toughness determination has been well reported in literature [23-24]. The composites were machined for the CNT testing with gauge length, specimen diameter (D), notch diameter (d), and notch angle of 30, 6, 4.5 mm, and 60 °C. The specimens were then subjected to tensile loading to fracture using an instron universal testing machine. The fracture load (P_f) obtained from the CNT specimens' load – extension plots were used to evaluate the fracture toughness using the empirical relations by Dieter [25]:

$$K_{1C} = P_f/(D)^{3/2}[1.72(D/d) - 1.27] \quad (2.3)$$

where, D and d are respectively the specimen diameter and the diameter of the notched section. The validity of the fracture toughness values was evaluated using the relations in accordance with Nath and Das [26]:

$$D \geq (K_{1C}/\sigma_y)^2 \quad (2.4)$$

Three repeat tests were performed for each composite composition and the results obtained were taken to be highly consistent if the difference between measured values for a given composite composition is not more than 2%.

2.7 Hardness Test

The hardness of the composites was evaluated using an Emco TEST DURASCAN Microhardness Tester equipped with ecos workflow ultra modern software. Prior to testing, test specimens cut out from each composite composition were polished to obtain a flat and smooth surface finish. A load of 100 g was applied on the specimens and the hardness profile was evaluated following standard procedures. Multiple hardness tests were performed on each sample and the average value taken as a measure of the hardness of the specimen.

2.8 Microstructural Examination

A Zeiss Metallurgical Microscope with accessories for image analysis was used for optical microscopic investigation of the composites produced. The specimens for the test were metallographic ally polished and etched with 1HNO3: 1HCl solution before microscopic examination was performed. A JSM 7600F Jeol ultra-high resolution field emission gun scanning electron microscope (FEG-SEM) equipped with an EDS (courtesy of the Department of Chemical and Metallurgical Engineering, Tshwane University of Technology, Pretoria, South Africa) was used for detailed study of the microstructural features and elemental compositions of the composites.

2.9 Corrosion Test

The corrosion behaviour of the composites was studied by weight loss method using mass loss and corrosion rate measurements as basis for evaluating the results generated. The corrosion test was carried out by immersion of the test specimens in 0.3M H_2SO_4 (pH 1.3) and 5wt% NaCl (pH 8.37) solutions which were prepared following standard procedures [7]. The specimens for the test were cut to size 15×15×10 mm and then mechanically polished with emery papers from 220 down to 600 grades to produce a smooth surface. The samples were de-greased with acetone, rinsed in distilled water, and then dried in air before immersion in still solutions of 0.3M H_2SO_4 and 5wt% NaCl at room temperature (25 ^oC). The solution-to-specimen surface area ratio was about 150 ml cm^{-2}, and the corrosion setups were exposed to atmospheric air for the duration of the immersion test. The weight loss readings were monitored on two day intervals for a period of 22 days. The mass loss (mg/cm^2) for each sample was evaluated in accordance with ASTM G31 standard recommended practice [27] following the relation:

$$m.l = CW/A \tag{2.5}$$

where m.l is the mass loss (mg/cm^2), CW is the cumulative weight loss (mg), and A is the total surface area of the sample (cm^2).

Corrosion rate for each sample was evaluated from the weight loss measurements following the relation [7]:

$$C.R = KW/\rho At \tag{2.6}$$

Where C.R is corrosion rate (mmy), W is weight loss (g), D is the density (g/cm^3), A is the area (cm^2), T is time (hours), and K is a constant equal to 87500.

$$W = W_i - W_f \tag{2.7}$$

where W is the weight loss (g), W_i is the initial weight (g) and W_f is the final weight (g).

Three repeat tests were carried out for each composition of the composite, and the reproducibility and repeatability were found to be good as there were no significant differences between results from triplicates.

3.0 RESULTS AND DISCUSSION

3.1 Microstructure

Representative optical and scan electron photomicrographs; and the EDAX profiles of the BLA-SiC reinforced Aluminium hybrid composites produced are presented in Figs 1-2. Figure 1 shows the optical photomicrographs of the Al-Mg-Si/2wt%BLA-8wt%SiC hybrid composite. It is observed that the reinforcing particles (BLA and SiC) are visible and clearly delineated in the microstructure. The particles are fairly well distributed in the Al-Mg-Si matrix and signs of particle clusters are minimal. Figure 2 shows secondary electron image and EDAX profile of the Al-Mg-Si/ 2wt% BLA-8wt%SiC hybrid composite. From Fig. 2(a) the reinforcing particles can be easily identified; the EDS profile of the composite (Fig. 2b) shows peaks of aluminium (Al), oxygen (O), carbon (C), iron (Fe), and silicon (Si). The presence of these elements confirms the presence of silicon carbide (SiC); silica (SiO_2), alumina (Al_2O_3), and ferric oxide (Fe_2O_3) in the composite. It is noted that silica (SiO_2), alumina (Al_2O_3), and ferric oxide (Fe_2O_3) observed in the EDAX profile are primary constituents found in bamboo leaf ash [18].

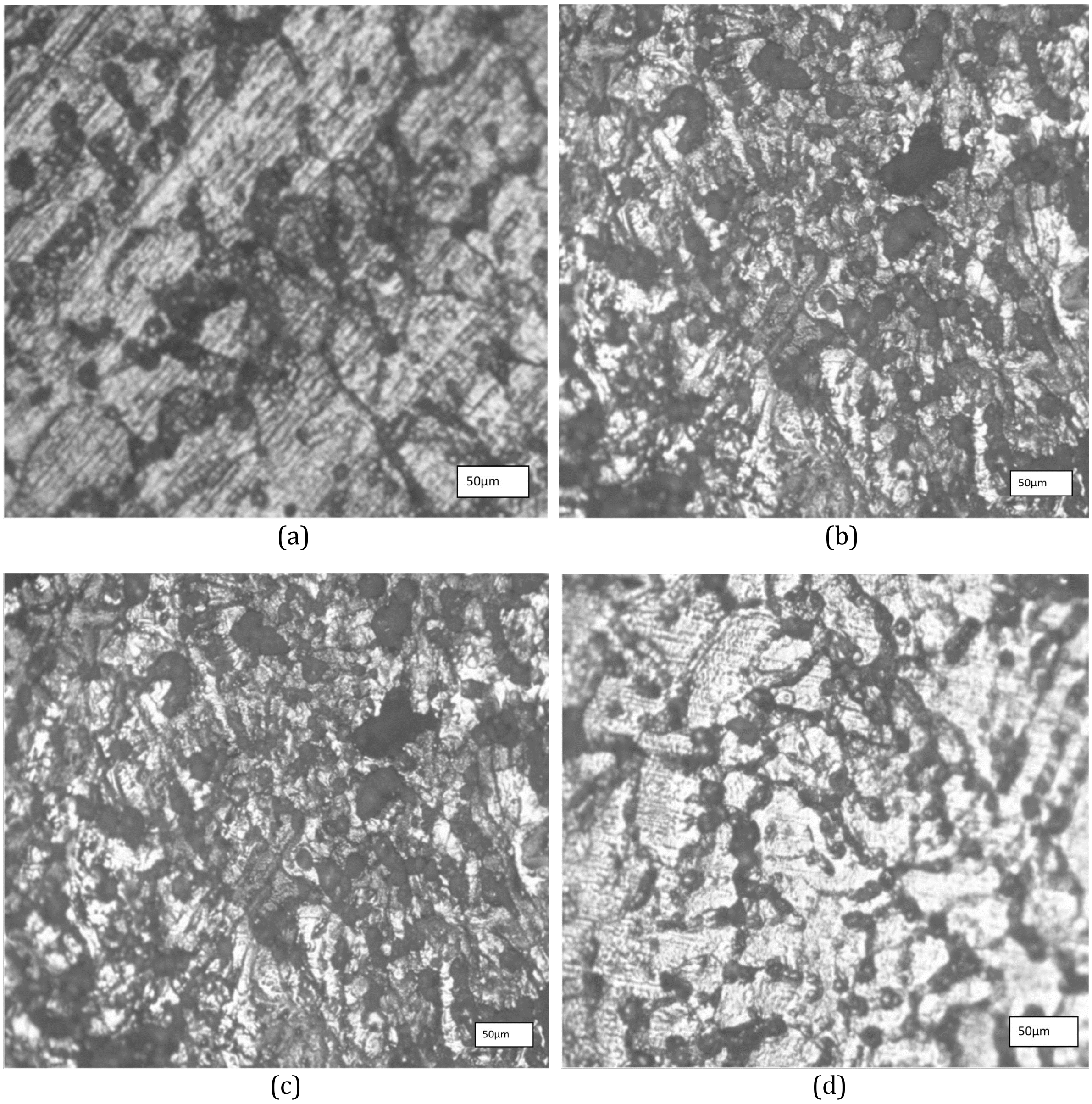

Fig. 1. Photomicrograph showing (a) Al-Mg-Si/10 wt% SiC composite with the SiC particles dispersed in the Al-Mg-Si matrix, (b) Al-Mg-Si/2wt% BLA-8 wt% SiC hybrid composite with the BLA-SiC particles dispersed in the Al-Mg-Si matrix, (c) Al-Mg-Si/3wt% BLA-7 wt% SiC hybrid composite showing the BLA-SiC particles dispersed in the Al-Mg-Si matrix, and (d) Al-Mg-Si/4wt% BLA-6 wt% SiC hybrid composite showing the BLA-SiC particles dispersed in the Al-Mg-Si matrix.

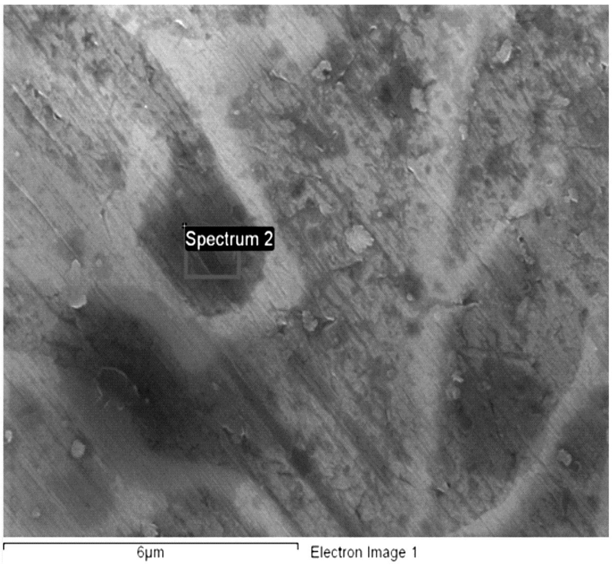

(a)

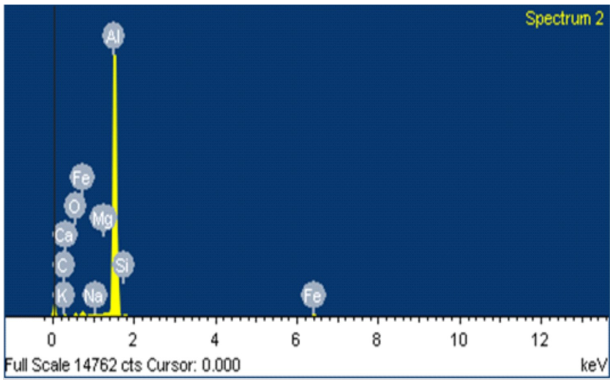

(b)

Fig. 2. (a) representative SEM Photomicrograph of the Al-Mg-Si/2wt% BLA-8 wt% SiC hybrid composite showing particles dispersed in the Al-Mg-Si matrix, and (b)EDAX profile obtained from the Al-Mg-Si/2wt% BLA-8 wt% SiC hybrid composite confirming the presence of SiC, Al_2O_3, SiO_2, Fe_2O_3, K_2O, and CaO.

Table 3. Composite density and estimated percent porosity.

Sample	Weight Ratio of BLA and SiC	Theor-etical Density	Experi-mental Density	% Porosi-ty
A	0:10	2.745	2.714	1.14
B	2:8	2.694	2.670	0.89
C	3:7	2.668	2.638	1.24
D	4:6	2.643	2.615	1.06

The results of the percent porosity of the composites are presented in Table 3. It is observed from comparison of the theoretical and experimental densities of the composites that slight porosities (less than 1.5%) exist in the produced composites. The use of BLA and SiC as complementing reinforcements in the Al matrix did not arise in any significant rise in porosity level of the hybrid composites when compared with the single reinforced Al - 10 wt% SiC composite. Porosity levels not above 4% have been reported to be acceptable in cast Aluminium matrix composites [19].

3.2 Mechanical Behaviour

The mechanical properties of the composites presented in Figs. 3 - 8. The hardness (Fig. 3), ultimate tensile strength (Fig. 4) and yield strength (Fig. 5) of the composites are observed to decrease with increase in BLA content in the composites. 4.58, 8.14, and 10.94% reduction in hardness , and 7.97, 15.6, and 23.29% reduction in ultimate tensile strength were observed for the hybrid composites having respectively 2, 3, and 4 wt% BLA in comparison with the single reinforced Al-Mg-Si matrix -10wt% SiC composite. This trend is due to the composition of the BLA which consists mainly of silica which is noted to have lower hardness and strength levels in comparison with silicon carbide [28].

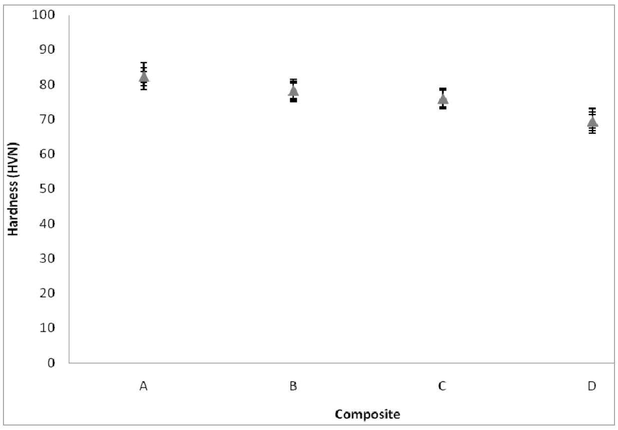

Fig. 3. Variation of Hardness for the single reinforced Al-Mg-Si/10 wt% SiC and hybrid reinforced Al-Mg-Si/BLA-SiC composites.

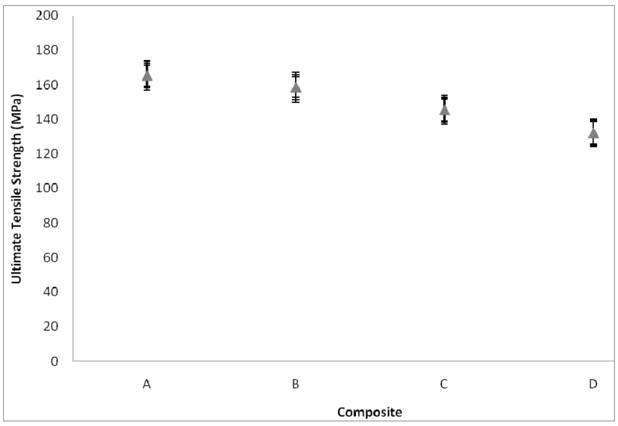

Fig. 4. Variation of Ultimate Tensile Strength for the single reinforced Al-Mg-Si/10 wt% SiC and hybrid reinforced Al-Mg-Si/BLA-SiC composites.

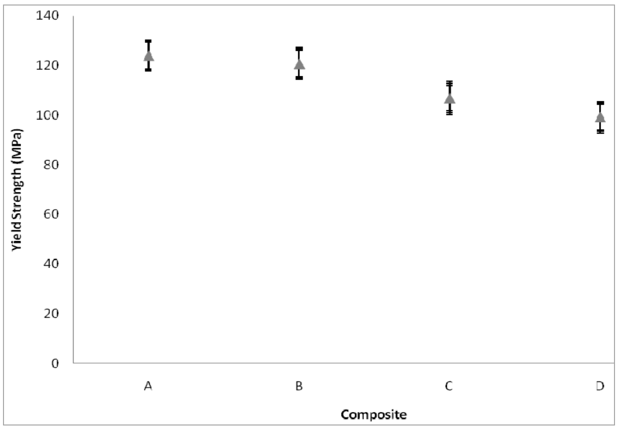

Fig. 5. Variation of Yield Strength for the single reinforced Al-Mg-Si/10 wt% SiC and hybrid reinforced Al-Mg-Si/BLA-SiC composites.

The specific strength (Fig. 6) and percent elongation (Fig. 7) are equally observed to decrease with increase in BLA content. In the case of the specific strength, it is noted that the margin of difference between the specific strength of the single reinforced Al-Mg-Si/10wt%SiC and the Al-Mg-Si/2wt%BLA-8wt%SiC is less than 2%. Also, the fracture toughness of the composites (Fig. 8) is observed to increase with increase in the BLA content, which is encouraging considering that MMCs are noted to have poor fracture toughness values. The fracture toughness values obtained were reported as plain strain fracture toughness because it meets the conditions specified by Das and Nath [26] and Alaneme and Aluko [5].The improvement in fracture toughness with increase in BLA content may be attributed to the increased presence of silica which is a softer ceramic in comparison with SiC. It is also noted that for most engineering materials fracture toughness scales inversely with yield strength [29] which is the case observed for the composites.

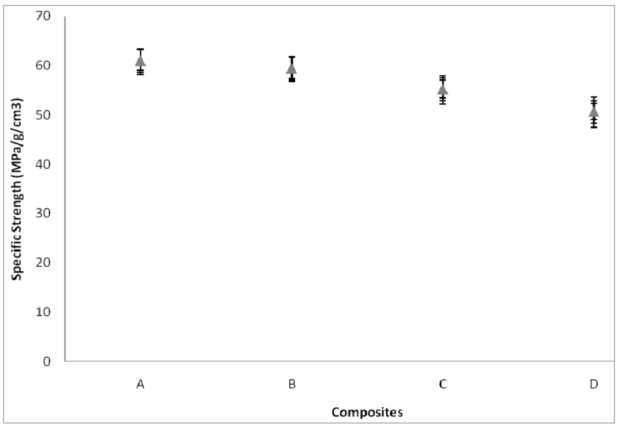

Fig. 6. Variation of Specific Strength for the single reinforced Al-Mg-Si/10 wt% SiC and hybrid reinforced Al-Mg-Si/BLA-SiC composites.

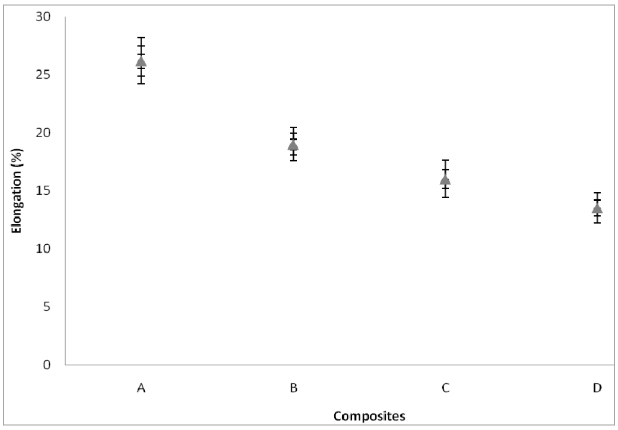

Fig. 7. Variation of Percent Elongation for the single reinforced Al-Mg-Si/10 wt% SiC and hybrid reinforced Al-Mg-Si/BLA-SiC composites.

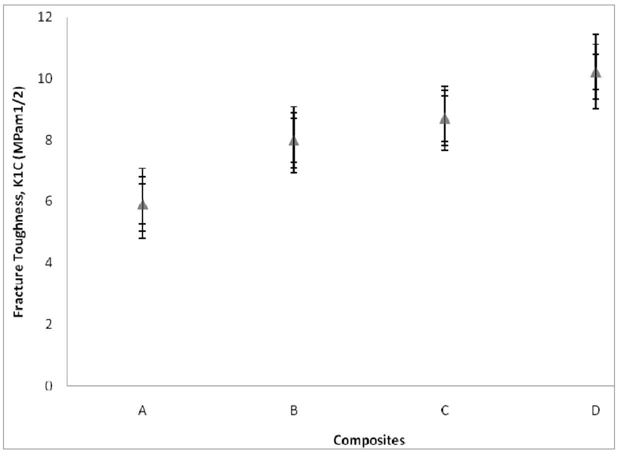

Fig. 8. Variation of Fracture Toughness for the single reinforced Al-Mg-Si/10 wt% SiC and hybrid reinforced Al-Mg-Si/BLA-SiC composites.

3.3 Corrosion Behaviour

Figure 9 show the variation of mass loss and corrosion rate with exposure time for composite samples immersed in 3.5% NaCl solution. From Fig. 9(a), it is observed that compared to sample A (Al-Mg-Si/10wt%SiC), sample B (Al-Mg-Si/2wt% BLA-8 wt% SiC) and sample C (Al-Mg-Si/3wt% BLA-7wt% SiC) had negative mass loss values for virtually the entire period of immersion in the 3.5% NaCl solution. The negative mass loss is indicative of weight gain during the period of immersion- suggesting that the passive film formed on sample B and C are very stable in comparison to that of sample A. Thus sample B (Al-Mg-Si/2wt% BLA-8 wt% SiC) and sample C (Al-Mg-Si/3wt% BLA-7wt% SiC) exhibits a higher resistance to corrosion in comparison to the single reinforced (Al-Mg-Si/10wt%SiC) composite. This trend in corrosion behaviour is supported by the corrosion rate profiles presented in Fig. 9(b). It is observed from the plot that peak corrosion was observed on the 3rd day of immersion with the 2 and 3 wt% BLA containing composites exhibiting the least susceptibility to corrosion. Bobic et al. [30] have reported on the corrosion susceptibility of Al matrix-SiC reinforced composites in marine (chloride) environments. The improvement in corrosion resistance observed by the addition of 2-3 wt% BLA is attributed to the presence of silica which is the primary constituent of BLA. Silica has been reported to inhibit the formation of Al_4C_3 phase which forms from interfacial reaction between the matrix and SiC during the production process [31]. The Al_4C_3 phase has been reported to have adverse effect on the corrosion resistance of aluminium based composites [32].

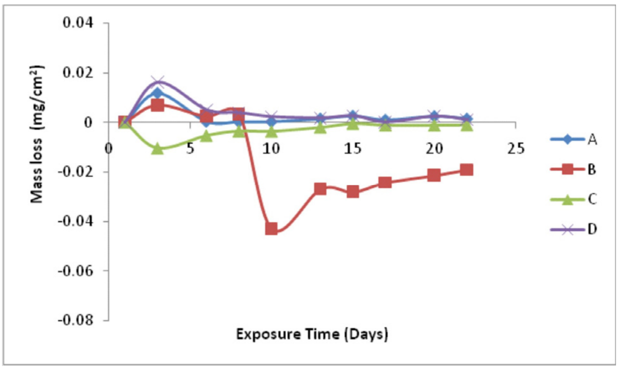

(a)

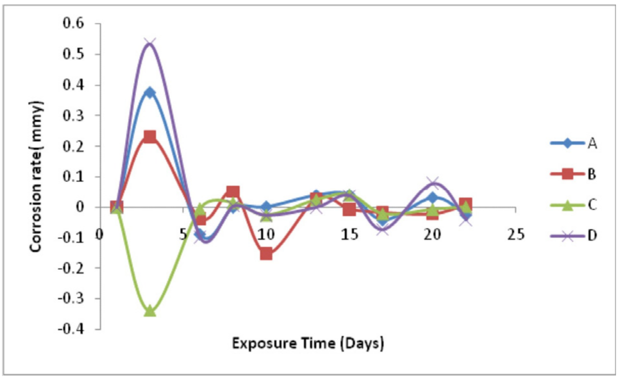

(b)

Fig. 9. Variation of (a) mass loss and (b) corrosion rate with exposure time for the single reinforced Al-Mg-Si/10 wt% SiC and hybrid reinforced Al-Mg-Si/BLA-SiC composites in 5wt% NaCl solution.

Figure 10 shows the plots of variation of mass loss and corrosion rate with exposure time for the composites immersed in 0.3 M H_2SO_4 solution. From Fig. 10(a), it is observed that the hybrid composites exhibit inferior corrosion resistance in comparison with the single reinforced Al-Mg-Si/10 wt% SiC composite (sample A). This is in contrast with the trend observed in 3.5% NaCl solution (Fig. 9). In addition, the mass loss increases with increase in exposure time. This is an indication that the passive film formed on the composites was unable to give adequate protection to the substrates; and the addition of BLA promoted corrosion of the composites. Furthermore it is observed that among the hybrid composites, the mass loss is more pronounced for the Al-Mg-Si/4wt%BLA-6wt%SiC composition. This same trend was also observed in 3.5% NaCl environment – an indication that the Al-Mg-Si/4wt%BLA-6wt%SiC composite composition may not be suitable for use in marine and acidic environments. Figure 10(b) shows that the corrosion rate behaviour of the composites is in agreement with the trends observed in Fig. 10(a).

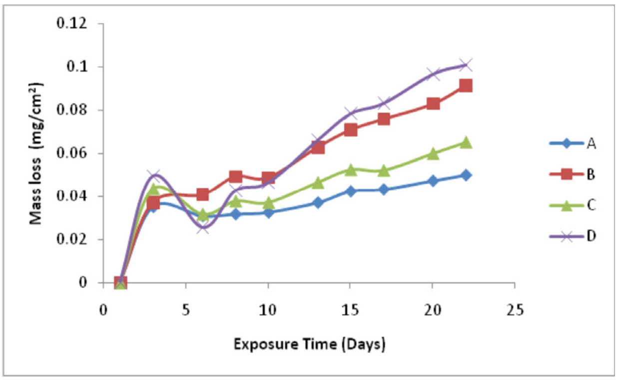

(a)

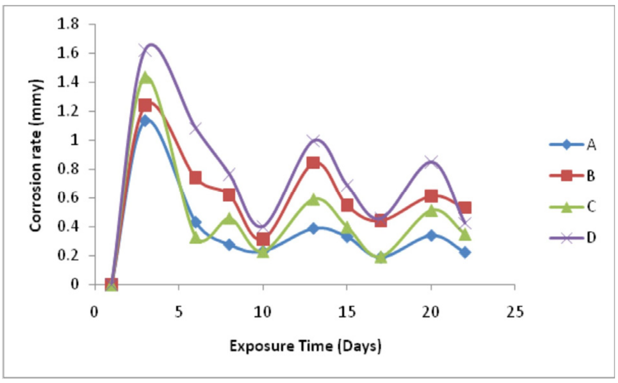

(b)

Fig. 10. Variation of (a) mass loss and (b) corrosion rate with exposure time for the single reinforced Al-Mg-Si/10 wt% SiC and hybrid reinforced Al-Mg-Si/BLA-SiC composites in 0.3M H_2SO_4 solution.

Figure 11 shows that the corrosion mechanism of the hybrid composites in H_2SO_4 solution is most likely to be galvanic corrosion as a result of the preferential dissolution of the Al matrix which exposed the BLA-SiC reinforcements. In this regards the Al matrix is known to have a higher electrochemical potential in comparison with BLA-SiC (ceramic particle) which have higher resistivity [33]. Thus at the Al matrix/reinforcement interfaces, micro galvanic corrosion cells are created which results in the dissolution of Al (anode) in preference to BLA-SiC (which serves as the cathode) [34-35].

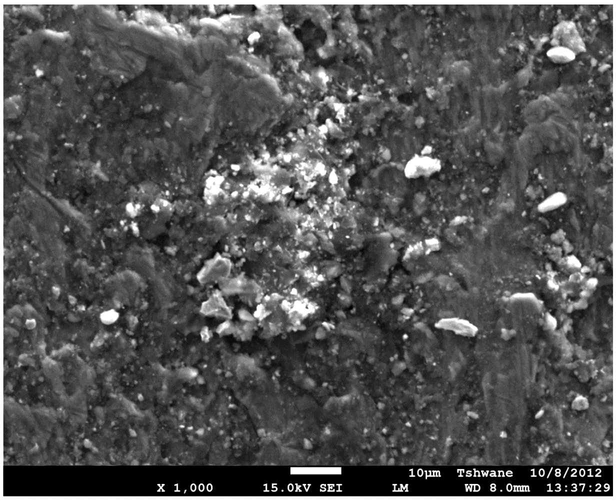

Fig. 11. SEM photomicrograph showing secondary electron image of the corroded surface of the Al-Mg-Si/3wt% BLA-7 wt% SiC hybrid composite.

3. CONCLUSION

The microstructures, mechanical properties and corrosion behaviour of Al-Mg-Si matrix composites containing 0:10, 2:8, 3:7, and 4:6 wt % bamboo leaf ash and silicon carbide as reinforcement was investigated. The results show that:

1. The hardness, ultimate tensile strength, and percent elongation of the hybrid composites decreased with increase in BLA content.
2. The fracture toughness of the hybrid composites was observed to be superior to that of the single reinforced Al - 10 wt% SiC composite.
3. The specific strength of the 2 wt % BLA containing hybrid composite was comparable to that of the single reinforced Al - 10 wt% SiC composite while the 3 and 4 wt % BLA containing hybrid composites had lower specific strength values.
4. In 5wt% NaCl solution, it was observed that the 2 and 3 wt % BLA containing hybrid composites had higher corrosion resistance in comparison to the single reinforced Al - 10 wt% SiC composite but the reverse trend was observed in 0.3M H2SO4 solution where the single reinforced Al - 10 wt% SiC composite had superior corrosion resistance.
5. The 4 wt % BLA containing hybrid composite composition was observed to be the least satisfactory in achieving the goal of reduced cost while maintaining high performance levels of the composites.

Acknowledgement

The authors acknowledge the assistance of Dr. P.A. Olubambi of the Department of Chemical and Metallurgical Engineering, Tshwane University of Technology, South Africa in carrying out microstructural and compositional characterization of the composites produced.

REFERENCES

[1] P. Rohatgi, B. Schultz: *Lightweight metal matrix nanocomposites – stretching the boundaries of metals*, Materials Matters, Vol. 2, pp. 16-19, 2007.

[2] K.K. Alaneme: *Mechanical Behaviour of Cold Deformed and Solution Heat-treated Alumina Reinforced AA 6063 Composites*, The West Indian Journal of Engineering, Vol. 35, No. 2, 2013 (In Press).

[3] M.K. Surappa: *Aluminium matrix composites: Challenges and opportunities*, Sadhana, Vol. 28, No. 1&2, pp. 319-34, 2003.

[4] D.B. Miracle: *Metal matrix composites - from science to technological significance,* Composites Science and Technology, Vol. 65, No. 15-16, pp. 2526-40, 2005.

[5] K.K. Alaneme, A.O. Aluko: *Fracture Toughness (K_{1C}) and Tensile Properties of As-Cast and Age-Hardened Aluminium (6063) – Silicon Carbide Particulate Composites,* Scientia Iranica, Vol. 19, No. 4, pp. 992 – 996, 2012.

[6] A. Macke, B.F. Schultz, P. Rohatgi: *Metal matrix composites offer the automotive industry an opportunity to reduce vehicle weight, improve performance*, Advanced Materials and Processes, Vol. 170, No. 30, pp. 19-23, 2012.

[7] K.K. Alaneme, M.O. Bodunrin: *Corrosion behaviour of alumina reinforced Al (6063) metal matrix composites*, Journal of Minerals and Materials Characterisation and Engineering, Vol. 10, No. 2, pp. 1153-65, 2011.

[8] S. Mitrović, M. Babić, B. Stojanović, N. Miloradović, M. Pantić, D. Džunić: *Tribological Potentials of Hybrid Composites Based on Zinc and Aluminium Alloys Reinforced with SiC and Graphite Particles*, Tribology in Industry, Vol. 34, No. 4, pp. 177-185, 2012.

[9] T.V. Christy, N. Murugan, S. Kumar: *A comparative study on the microstructures and mechanical properties of Al 6061 alloy and the MMC Al 6061/TiB2/12p*, Journal of Minerals and Materials Characterization and Engineering, Vol. 9, No. 1, pp. 57–65, 2010.

[10] S. Valdez, B. Campillo, R. Perez, L. Martinez, H. Garcia: *Synthesis and microstructural characterization of Al-Mg alloy-SiC particulate composite*, Materials Letters, Vol. 62, No. 17-18, pp. 2623-2625, 2008.

[11] P.B. Madakson, D.S. Yawas, A. Apasi: *Characterization of Coconut Shell Ash for Potential Utilization in Metal Matrix Composites for Automotive Applications*, International Journal of Engineering Science and Technology (IJEST), Vol. 4, No. 3, pp. 1190-1198, 2012.

[12] K.V. Mahendra, A. Radhakrisna: *Characterization of stir cast Al-Cu-(fly ash + SiC) hybrid Metal Matrix Composites*, Journal of Composite Materials, Vol. 44, No. 8, pp. 989-1005, 2010.

[13] H. Zuhailawati, P. Samayamutthirian, C.H. Mohd Haizu, *Fabrication of Low Cost Aluminium Matrix Composite Reinforced with Silica Sand*, Journal of Physical Science, Vol. 18, No. 1, pp. 47–55, 2007.

[14] F.C.R. Hernandez, H.A. Calderon, *Nanostructured Al/Al4C3 composites reinforced with graphite or fullerene and manufactured by mechanical milling and spark plasma sintering*, Materials Chemistry and Physics, Vol. 132, No. 2-3, pp. 815-822, 2012.

[15] K.K. Alaneme, I.B. Akintunde, P.A. Olubambi, T.M. Adewale: *Mechanical Behaviour of Rice Husk Ash – Alumina Hybrid Reinforced Aluminium Based Matrix Composites*, Journal of Materials research and Technology, 2012 (In Press).

[16] S.D. Prasad, R.A. Krishna: *Tribological Properties of A356.2/RHA Composites*, Journal of Materials Science and Technology, Vol. 28, No. 4, pp. 367-372, 2012.

[17] S.D. Prasad, R.A. Krishna: *Production and Mechanical Properties of A356.2 /RHA Composites*, International Journal of Advanced Science and Technology, Vol. 33, pp. 51-58, 2011.

[18] O.A. Olugbenga, A.A. Akinwole: *Characteristics of Bamboo Leaf Ash Stabilization on Lateritic Soil in Highway Construction*, International Journal of Engineering and Technology, Vol. 2, No. 4, pp. 212-219, 2010.

[19] K.K. Alaneme, A.O. Aluko: *Production and age-hardening behaviour of borax pre-mixed SiC reinforced Al-Mg-Si alloy composites developed by double stir casting technique*, The West Indian Journal of Engineering, Vol. 34, No. 1-2, pp. 80 – 85, 2012.

[20] K.K. Alaneme: *Influence of Thermo-mechanical Treatment on the Tensile Behaviour and CNT evaluated Fracture Toughness of Borax premixed SiCp reinforced Aluminium (6063) Composites*, International Journal of Mechanical and Materials Engineering, Vol. 7, No. 1, pp. 96 – 100, 2012.

[21] ASTM E 8M: Standard Test Method for Tension Testing of Metallic Materials (Metric), Annual Book of ASTM Standards, Philadelphia, 1991.

[22] K.K. Alaneme: *Fracture toughness (K_{1C}) evaluation for dual phase low alloy steels using circumferential notched tensile (CNT) specimens*, Materials Research, Vol. 14, No. 2, pp. 155-160, 2011.

[23] A. Bayram, A. Uguz, A. Durmus: *Rapid Determination of the Fracture Toughness of Metallic Materials Using Circumferentially Notched Bars*, Journal of Materials Engineering and Performance, Vol. 11, No. 5, pp. 571-576, 2002.

[24] D.M. Li, A. Bakker: *Fracture Toughness Evaluation Using Circumferentially-Cracked Cylindrical bar Specimens*, Engineering Fracture Mechanic, Vol. 57, pp. 1-11, 1997.

[25] G.E. Dieter. Mechanical Metallurgy, McGraw-Hill, Singapore; 1988.

[26] S.K. Nath, U.K. Das: *Effect of microstructure and notches on the fracture toughness of medium carbon steel*, Journal of Naval Architecture and Marine Engineering, Vol. 3, pp. 15-22, 2006.

[27] ASTM G31 Standards: Metals Test Methods and Analytical Procedures, Vol. 3, Wear and Erosion; Metal Corrosion, Annual Book of ASTM Standards, Philadelphia, 1994.

[28] T.W. Courtney: Mechanical Behaviour of Materials, Second Edition, Overseas Press, India, 2006.

[29] K.K. Alaneme, S.M. Hong, I. Sen, E. Fleury, U. Ramamurty: *Effect of Copper Addition on the Fracture and Fatigue Crack Growth Behaviour of Solution Heat-treated SUS 304H Austenitic Steel*, Materials Science and Engineering: A, Vol. 527, No. 18-19, pp. 4600 – 4604, 2010.

[30] B. Bobic, S. Mitrovic, M. Bobic, I. Bobic: *Corrosion of Metal Matrix Composites with Aluminium Alloy Substrate*, Tribology in Industry, Vol. 32, No. 1, pp. 3-11, 2010.

[31] K.K. Alaneme: Corrosion Behaviour of heat-treated Al-6063/ SiC_p Composites immersed in 5wt% NaCl Solution, Leonardo Journal of science, Vol. 18, pp. 55 – 64, 2011.

[32] R. Escalera-Lozano, C. Gutierrez, M.A. Pech-Canul, M.I. Pech-Canul: *Degradation of Al/SiCp Composites produced with Rice-Hull Ash and Aluminium Cans*, Waste Management, Vol. 28, pp. 389-395, 2008.

[33] G.M. Pinto, N. Jagannath, A.N. Shetty: *Corrosion Behavior of 6061 Al-15 vol. pct. SiC Composite and its Base Alloy in Mixture of 1:1 Hydrochloric and Sulphuric Acid Medium*, International Journal of Electrochemical Science, Vol. 4, pp. 1452-1468, 2009.

[34] K.K. Alaneme: *An Investigation on the Influence of SiC Volume Percent and Heat-Treatment on the Corrosion Behaviour of Al-6063/ SiC_p Composites in HCl - H_2SO_4 Environment*, Nigerian Society of Engineers Technical Transactions, Vol. 46, No. 1, pp. 13 – 25, 2011.

[35] B. Bobic, S. Mitrovic, M. Bobic, I. Bobic: *Corrosion of Aluminium and Zinc-Aluminium Alloys based Metal Matrix Composites*, Tribology in Industry, Vol. 31, No. 3 & 4, pp. 44-54, 2009.